



CrossMark  
 click for updates

Cite this: *RSC Adv.*, 2015, 5, 96990

# Isomerization of hexoses from enzymatic hydrolysate of poplar sawdust using low leaching $K_2MgSiO_4$ catalysts for one-pot synthesis of HMF

Xiang Shen,<sup>ab</sup> Yanxin Wang,<sup>\*c</sup> Birgitte K. Ahring,<sup>\*a</sup> Hanwu Lei,<sup>a</sup> Qiang Gao<sup>b</sup> and Hui Liu<sup>c</sup>

A cost-effective  $K_{1.5}Mg/SiO_2$  catalyst with a  $K_2MgSiO_4$  component was employed to help transfer several hexoses into hydroxylmethylfurfural (HMF) in a biphasic water/butanol system. The solid catalysts with rod-like structures and moderate base sites could promote the aldose–ketose isomerization of glucose and have potential for the synthesis of lactic acid *via* a retro-aldol condensation. In the presence of sulfonated titania/mordenite solid acid, the  $K_{1.5}Mg/SiO_2$  catalyst presented heat-stability and prolonged activity in the one-pot conversion of glucose to HMF, leading to an optimal yield of 62.2%. The one-pot catalysis of saccharides from the enzymatic hydrolysate of poplar sawdust achieved a high HMF yield of 56.9% at a glucose conversion of 91.6%.

Received 24th August 2015  
 Accepted 26th October 2015

DOI: 10.1039/c5ra17132f

[www.rsc.org/advances](http://www.rsc.org/advances)

## Introduction

Current agricultural and forestry residues and municipal solid waste including abundant lignocellulosic biomass could provide low cost and sustainable resources for the production of various valuable chemicals containing HMF.<sup>1–3</sup> Among these options, intensively-grown poplars have gained great attention in the midwestern United States due to continuously increasing productivity and cold/drought tolerance.<sup>4,5</sup> Enzymatic hydrolysis of poplars can produce various sugars, followed by fermentation to fuel-grade ethanol. The treatment with enzymes, bacteria, and fungi<sup>6,7</sup> took place in mild conditions and spotlighted on their potential to simplify and improve key process steps *via* modern biotechnology. In fact, as main components of lignocellulosic biomass, hemicellulose was formed by the linkage of five different sugar monomers of D-xylose, L-arabinose, D-galactose, D-mannose, and D-glucose,<sup>8,9</sup> and cellulose consisted of D-glucose linked by 1,4-β-glycosidic bonds.<sup>10,11</sup> The pretreatment operation,<sup>12</sup> such as steam explosion, ammonia fiber expansion, aqueous ammonia recycle, dilute sulfuric acid, lime, and sulfite had to be applied prior to the biological steps to overcome the natural recalcitrance from lignin sheath and cellulose. However, several problems derived

from the hydrolysate with a broad range of compounds having inhibitory effects on the microorganisms for subsequent fermentation, the pentoses being difficult to ferment, and least flexibility to treat different raw materials. For these reasons, there is a great interest in developing new catalytic technologies.<sup>13–15</sup> The route to effectively hydrolyze lignocellulosic biomass by integrating solid base and acid catalysts could easily overcome above-mentioned problems.

As an important intermediate, HMF can be produced from glucose by heterogeneous catalysis,<sup>16–18</sup> which would be used for biodegradable surfactants, pharmaceuticals, furanic polyesters, polyamides, and biofuels.<sup>19–22</sup> However, glucose only contained 1% of furanose tautomers in aqueous solutions, which gave poor HMF yield in direct dehydration due to side reactions. Integrating isomerization of hexose to ketose and subsequent ketose dehydration to HMF was considered as an effective method. For this purpose, some research teams focused on combining metal chloride salts (*e.g.*,  $AlCl_3$ ,  $CrCl_3$ ,  $SnCl_4$ ,  $LaCl_3$ ) with a Brønsted acid (*e.g.* HCl) to perform the glucose isomerization/dehydration reactions, leading to high HMF yield of 67 mol%.<sup>23,24</sup> However, metal halides were generally inactive in neutral aqueous solution, the use of strong mineral acids incurred environmental problems, and the separation of HMF was difficult. Interestingly, Davis group found that a Sn-beta zeolite could isomerize glucose to fructose with high activity in water under acidic conditions.<sup>25,26</sup> The unique performance of the Sn-beta solid Lewis acid created new opportunities for the facile integration of isomerization with dehydration steps. Nikolla group<sup>27</sup> developed the synergistic catalysis of Sn-beta with HCl for glucose conversion in a water/butanol biphasic system, leading to 55 mol% HMF selectivity under a glucose conversion of 75%. However, Sn-beta is not a commercially

<sup>a</sup>Bioproducts Science and Engineering Laboratory, Washington State University, Richland, WA 99352, USA. E-mail: [bka@tricity.wsu.edu](mailto:bka@tricity.wsu.edu); [hlei@tricity.wsu.edu](mailto:hlei@tricity.wsu.edu); Fax: +1 5093726782; Tel: +1 5093726782

<sup>b</sup>Engineering Research Center of Nano-Geo Materials of Ministry of Education, China University of Geosciences, Wuhan 430074, China. E-mail: [xiang.shen@tricity.wsu.edu](mailto:xiang.shen@tricity.wsu.edu)

<sup>c</sup>State Key Laboratory of Biogeology and Environmental Geology & School of Environmental Studies, China University of Geosciences, Wuhan 430074, China. E-mail: [yx.wang@cug.edu.cn](mailto:yx.wang@cug.edu.cn)

available zeolite and complex preparation leading to high cost. In addition, the enzymatic hydrolysate of poplar sawdust included glucose, cellobiose, xylose, mannose, and galactose; efficient conversion of these saccharides to HMF will be a substantial challenge.

Given the fact, the work focused on the aldose–ketose isomerization using low leaching solid catalysts for improving the selectivity of HMF in a one-pot system. A combination of sulfonated titania/mordenite (TM) with different  $K_xMg/SiO_2$  catalysts could afford high HMF yield under a moderate reaction temperature. The one-pot reaction using heterogeneous catalysts would provide the best solution to process the complex saccharides from poplar sawdust.

## Experimental

### Preparation and characterization of solid catalysts

The optimal titania/mordenite solid-acid was prepared by sol-gel-hydrothermal method according to our previous report.<sup>28</sup> The sulfonated titania/mordenite catalysts were denoted as  $TM_{0.2-0.5}$  (ratio of mordenite to titania is 20, 30, 40 and 50 wt%, respectively).

The  $K_xMgSiO_4$  catalysts were prepared by precipitation-gel method. In a typical procedure, 8.8 g of  $Mg(NO_3)_2 \cdot 6H_2O$  and 0.3 g CTAB was dissolved with 10 mL mixed solution of deionized water and ethanol (50% by volume). The solution was added into 20 mL acidic industrial silica sol (31 wt%  $SiO_2$ , pH of 3) under vigorous stirring for 15 minutes. The stoichiometric potassium carbonate was dissolved with about 10 mL deionized water and added into the above mixed sol under homogeneously stirring for 30 minutes. The forming gel was aged overnight at 403 K and then washed with ethanol. The resultant precursors were dried and calcined at 973 K for 2 h. Thermally activated catalysts were denoted as  $K_xMg/SiO_2$  (as K/Si molar ratio,  $x = 1.0, 1.2, 1.5, 1.7$ ).

The microstructure of prepared solid catalysts was analyzed by a FEI Sirion 200 field emission scanning electron microscope (FESEM), FEI Tecnai G2 20 Transmission Electron Microscope (TEM) and X'Pert PRO DY2198 X-ray diffractometer (XRD). The mean crystallite size of samples was calculated by the XRD line width of 220 peak using the Scherrer formula. The alkalinity of samples was studied with TPD using  $CO_2$  as molecular probe. Each sample was treated at 573 K with  $N_2$  flow of  $30 mL min^{-1}$  for 1 h and then in a reacting  $CO_2$  flow of  $15 mL min^{-1}$  at 323 K for 30 min. The physical adsorbed  $CO_2$  was eliminated by pure nitrogen. The oven temperature of the TPD was programmed from 323 K to 1073 K at  $10^\circ C min^{-1}$  in He flow of  $15 mL min^{-1}$  and desorbed  $CO_2$  was detected using TP-5075 apparatus (Tianjin Xianquan Co.) with thermal conductivity detector. The potassium and magnesium analyses were carried out by using inductively coupled plasma-atomic emission spectrometer (Thermo IRIS Interpid XSP ICP-AES, USA). Refer to digestion procedure, about 0.1 g catalyst sample was transferred into a Teflon vessel containing 5 mL hydrochloric acid (37%) and heated on a hot plate at  $120^\circ C$  until the residual liquid was 2–3 mL. Next, 5 mL nitric acid (69%) was added into the Teflon vessel to obtain colorless solution by evaporation, followed by

drying at the same temperature by the addition of 2 mL hydrofluoric acid (40%). At last, 2 mL nitric acid was added to dissolve the residue. As an analytical sample, 0.1 mL of the digestion solution was suctioned with a pipette into a volumetric flask to 25 mL by addition of ultra pure water. Blank tests and parallel experiments were conducted to improve the measurement accuracy and precision. Thermogravimetric analysis (TG) and differential thermal analysis (DTA) was carried out on a PerkinElmer Diamond TG/DTA instrument from 25 to  $500^\circ C$  at a ramp of  $10^\circ C min^{-1}$  under a flow of  $N_2$  for evaluating the thermal stability of prepared catalysts.

### Catalytic tests

In order to achieve fast separation of product and reactants, one-pot catalysis of saccharides from the enzymatic hydrolysate of poplar sawdust was performed in water/butanol biphasic system using a 250 mL thick-walled glass reactor under nitrogen ( $20 mL min^{-1}$ ) with a reflux-condenser. An oil bath was used to heat the reactor rapidly to the desired reaction temperature, with temperature and stirring being controlled by a digital laboratory hot plate magnetic stirrer (IKA<sup>TM</sup> RCT Basic IKAMAG<sup>TM</sup> Safety Control). In a typical experiment,  $K_xMgSiO_4$  catalyst of 0.4 g and 10 mL saccharides solution (or 0.6 g glucose dissolved in 10 mL saturated sodium chloride solution) were transferred to the reactor and then poured 30 mL butanol into it. The reactor was immersed in the oil bath of  $120^\circ C$  and stirred at 600 rpm for 1 h. Next, 0.6 g solid-acid was added to the reaction system at  $140^\circ C$  for 2 h. The reaction was quenched by soaking the reactor in ice water. The resultant aqueous and organic phases were separated for subsequent analysis. The determination of HMF, organic acids and saccharides was performed by Dionex UltiMate 3000 high performance liquid chromatography system (HPLC) equipped with Aminex HPX-87H Column ( $9 \mu m, 300 \times 7.8 mm$ ) and Dionex Refractive Index (RI) detector at  $65^\circ C$ . The mobile phase was 5 mM sulfuric acid at a flow rate of  $0.6 mL min^{-1}$ . Each sample was diluted with ultrapure water of pH 5–7 before analysis. Glucose conversion and HMF yield were calculated from the product of the aqueous and organic phase concentration obtained by above test and their corresponding volumes after reaction since the value of  $V_{org}/V_{aq}$  was changed after reaction. The conversion of glucose was defined as the moles of glucose reacted divided by the moles of initial glucose; the selectivity of HMF was defined as the moles of HMF produced divided by the moles of glucose reacted; and the yield of HMF was defined by integrating the product of the glucose conversion and the HMF selectivity.

## Results and discussion

### Composition and surface properties of solid alkali

The characteristic diffraction peaks of crystalline  $K_2MgSiO_4$ , (220), (311), (400) and (422) at *ca.*  $2\theta = 32.77, 38.65, 47, 58.41$ , respectively, were observed in the X-ray patterns (Fig. 1). As the K/Si mole ratio increased, the peak of amorphous silica diminished whereas  $K_2MgSiO_4$  characteristic peaks significantly enhance, implying a change in composition and structure of

catalysts due to the addition of potassium carbonate. Another, it seemed that small amount of active component of the catalysts was  $\text{KNO}_3$  ((021), (012), (112), (221), (041) and (313) at *ca.*  $2\theta = 23.92, 29.49, 33.93, 41.3, 41.97, 68.76$ ) and  $\text{K}_2\text{O}$  ((220) and (700) at *ca.*  $2\theta = 19.81, 40.44$ ). This could be because the clustering or unevenly dispersed  $\text{KNO}_3$  on the catalyst formed in the hydrothermal process and only part of the loaded  $\text{KNO}_3$  decomposed into  $\text{K}_2\text{O}$  ((220), (700) at *ca.*  $2\theta = 19.81, 40.44$ ) under the thermal activation condition.<sup>29</sup> The characteristic diffraction peaks of silica and magnesia were not found, implying the formation of new active component of  $\text{K}_2\text{MgSiO}_4$  by the precipitation-gel process.

To provide additional evidence, morphologies of prepared catalysts were analyzed. The TEM images of  $\text{K}_{1.5}\text{Mg}/\text{SiO}_4$  showed rodlike crystal (Fig. 2f–h) and exhibited small round-shape particles on the surface (Fig. 2e). Comparing with Fig. 2c and i scanning micrograph, it could be seen that the crystalline particles decreased gradually with the increase of potassium amount in prepared catalysts. Electron micrographs (Fig. 2b, d, f and k) showed that the  $\text{K}_{1.5}\text{Mg}/\text{SiO}_2$  catalysts presented a cluster of well-developed rodlike structure with a certain length–diameter ratio different from other catalysts, implying a difference in catalytic activity owing to their different composition. And the  $\text{K}_{1.5}\text{Mg}/\text{SiO}_2$  catalysts can be well dispersed in reaction medium, which would be beneficial to the one-pot reaction. We noted that the  $\text{K}_{1.5}\text{Mg}/\text{SiO}_2$  catalyst with lower amount led to incomplete crystallization and an unclear image (Fig. 2a), implying an unmatched synergism between the active components and the silica support. Another, too much potassium loading could increase the moisture absorbency of prepared  $\text{K}_{1.7}\text{Mg}/\text{SiO}_2$  catalysts leading to agglomerated particles.

Advancing a step, we investigated  $\text{CO}_2$ -TPD profiles (Fig. 3) to validate the correlation between composition of prepared catalysts and their alkalinities. The broadening peaks corresponding to different temperature demonstrate the different basic sites on the surface of catalysts. The desorption peaks at about 373 K or 573 K demonstrated the moderate basic sites on

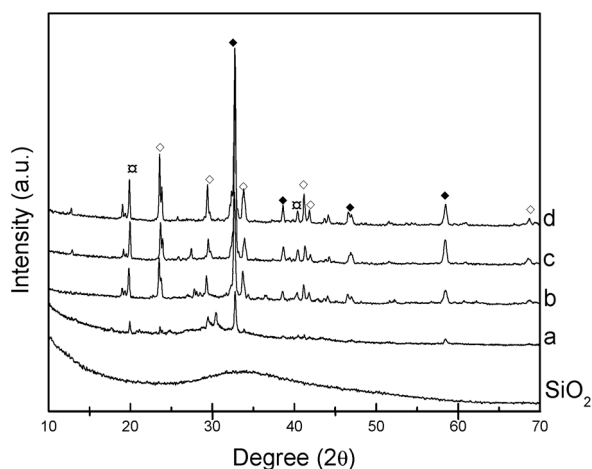


Fig. 1 XRD patterns of prepared solid bases: (a)  $\text{K}_{1.0}\text{Mg}/\text{SiO}_2$ , (b)  $\text{K}_{1.2}\text{Mg}/\text{SiO}_2$ , (c)  $\text{K}_{1.5}\text{Mg}/\text{SiO}_2$ , (d)  $\text{K}_{1.7}\text{Mg}/\text{SiO}_2$ ; (◇)  $\text{KNO}_3$ , (◆)  $\text{K}_2\text{MgSiO}_4$ , (○)  $\text{K}_2\text{O}$ .

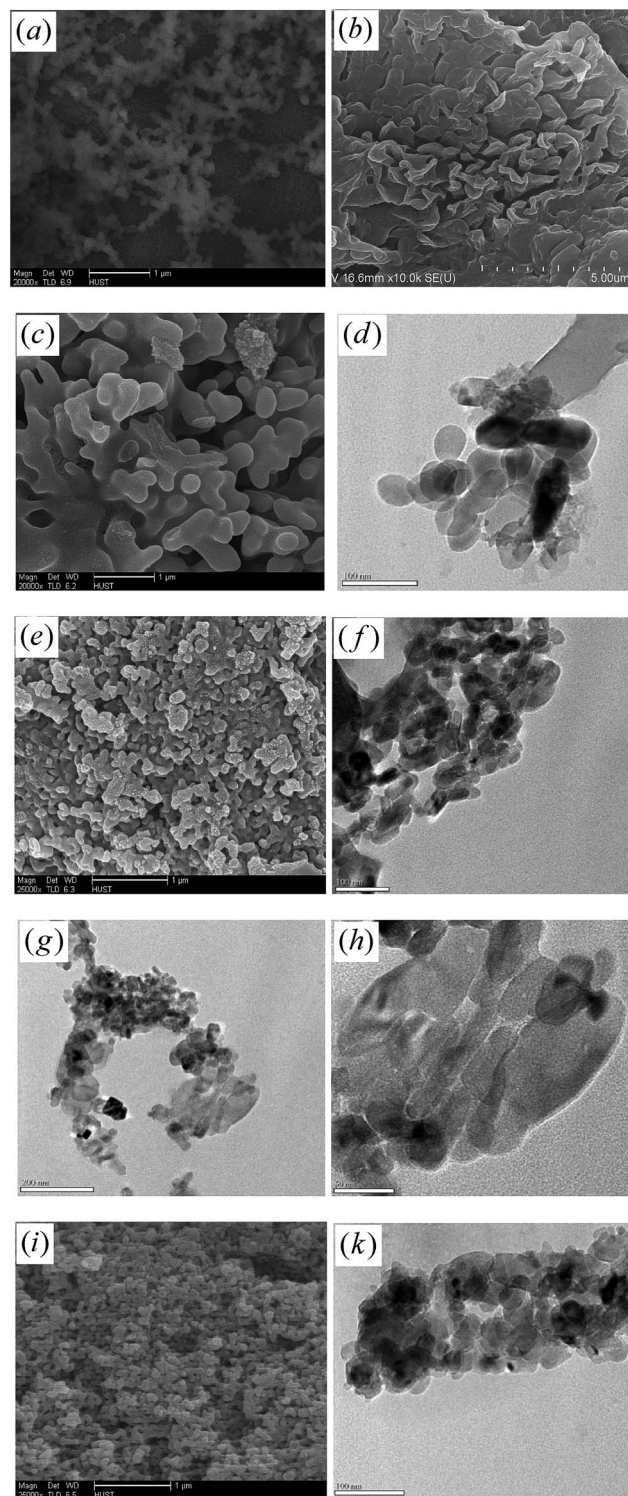


Fig. 2 FESEM images of prepared solid catalysts: (a)  $\text{K}_{1.5}\text{Mg}/\text{SiO}_2$  with a lower magnesium amount, (b)  $\text{K}_{1.0}\text{Mg}/\text{SiO}_2$ , (c)  $\text{K}_{1.2}\text{Mg}/\text{SiO}_2$ , (e)  $\text{K}_{1.5}\text{Mg}/\text{SiO}_2$  and (i)  $\text{K}_{1.7}\text{Mg}/\text{SiO}_2$ ; TEM (nm scale) images: ((d) 100 nm)  $\text{K}_{1.2}\text{Mg}/\text{SiO}_2$ , ((f) 100 nm, (g) 50 nm, (h) 200 nm)  $\text{K}_{1.5}\text{Mg}/\text{SiO}_2$  and ((k) 100 nm)  $\text{K}_{1.7}\text{Mg}/\text{SiO}_2$ .

the catalysts, which are associated with the surface  $\text{OH}^-$  groups adsorbed on the  $\text{K-O}$  or  $\text{Mg-O}$  species.<sup>30,31</sup> The  $\text{K}_2\text{MgSiO}_4$  component of catalyst would be the source of the moderate

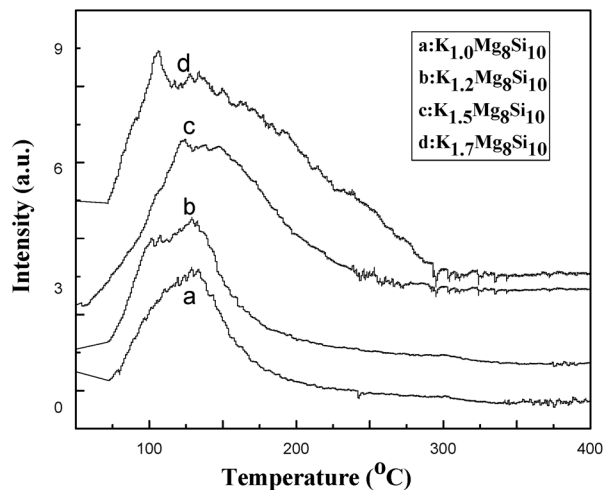


Fig. 3 CO<sub>2</sub>-TPD profiles of prepared solid catalysts: (a) K<sub>1.0</sub>Mg/SiO<sub>2</sub>, (b) K<sub>1.2</sub>Mg/SiO<sub>2</sub>, (c) K<sub>1.5</sub>Mg/SiO<sub>2</sub>, (d) K<sub>1.7</sub>Mg/SiO<sub>2</sub>.

basicity, which would induce excellent catalytic activity. Nevertheless, excess KNO<sub>3</sub> adsorbed on the catalyst could increase the moisture absorbency of prepared K<sub>1.7</sub>Mg/SiO<sub>2</sub> catalysts leading to agglomerated particles, which is unfavourable to the isomerization reaction.

### Catalytic activities

Saccharides conversion studies were carried out at 140 °C by integrating TM solid-acid and K<sub>x</sub>Mg/SiO<sub>2</sub> catalysts in a water/butanol biphasic system under the atmosphere of nitrogen. The composition of saccharides solution (pH of *ca.* 5) from enzymatic hydrolysate of poplar sawdust included glucose of 46.96 g L<sup>-1</sup>, cellobiose of 3.81 g L<sup>-1</sup>, xylose of 6.49 g L<sup>-1</sup>, mannose of 1.11 g L<sup>-1</sup> and galactose of 0.87 g L<sup>-1</sup>. Several chemicals such as acetic acid of 14.88 g L<sup>-1</sup> and furfural of 2.26 g L<sup>-1</sup> from the enzymatic process were also found. Fig. 4 depicts distribution of products for the conversion of saccharides to HMF by combining anhydrous AlCl<sub>3</sub> with different TM catalysts. It was noted that the glucose conversion was low, which could be resulted from inactive AlCl<sub>3</sub> under pH of 5 and oligosaccharides coating on the surface of catalysts. In the presence of the same Lewis acid, TM<sub>0.3</sub> catalysts showed a higher activity comparing to other TM catalysts. It also found that nearly all arabinose, galactose, and furfural disappeared due to forming water soluble and humic species. Interestingly, amount of acetic acid dropped sharply, indicating that acetic acid could facilitate the side reactions leading to humic and oligomeric species (Fig. 4).

In order to mitigate the negative effect of oligosaccharides and acetic acid, we chose the low concentration of enzymatic hydrolysate for the same reaction using TM<sub>0.3</sub> solid-acid and different K<sub>x</sub>Mg/SiO<sub>2</sub> catalysts. The composition of saccharides solution included glucose of 19.57 g L<sup>-1</sup>, acetic acid of 3.59 g L<sup>-1</sup>, cellobiose of 1.44 g L<sup>-1</sup>, xylose of 3.28 g L<sup>-1</sup>, mannose of 0.86 g L<sup>-1</sup> and furfural of 1.32 g L<sup>-1</sup>. The yield of HMF was significantly improved (Table 1). Moreover, the competitive adsorption was weakened due to less reactant molecules at

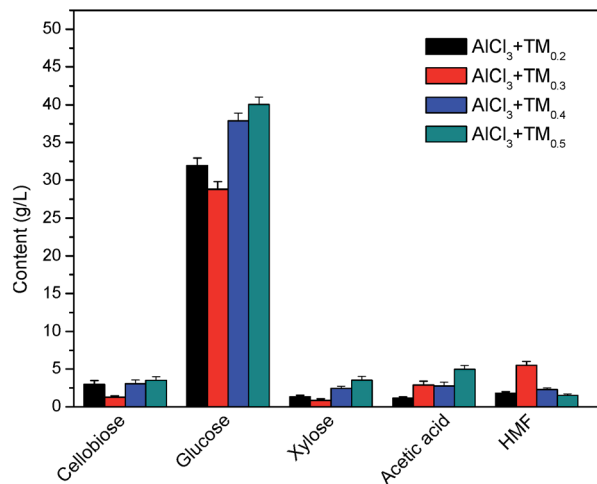


Fig. 4 Composition of products resulted from the conversion of saccharides from poplar sawdust by employing AlCl<sub>3</sub> with different TM solid acids; reaction conditions: 10 mL of saccharides solution (pH ≈ 5) at 140 °C for 180 min using 4 wt% anhydrous AlCl<sub>3</sub> and 6 wt% TM catalysts; organic to aqueous volume ratio of 3.

relatively low concentration, which could improve the interaction of active sites on catalysts with reactants. Considering the similar conditions, the catalytic activity corresponding to HMF yield increased as follows: K<sub>1.0</sub>Mg/SiO<sub>2</sub> < K<sub>1.2</sub>Mg/SiO<sub>2</sub> < K<sub>1.7</sub>Mg/SiO<sub>2</sub> < K<sub>1.5</sub>Mg/SiO<sub>2</sub>. Therefore, it was reasonable to assume that the moderate base sites played a significant role in determining the conversion of hexoses to HMF.

Furthermore, we conducted the conversion of glucose to HMF by integrating different K<sub>x</sub>Mg/SiO<sub>2</sub> catalyst with TM<sub>0.3</sub> catalysts (Fig. 5). The HMF selectivity increased with increasing glucose conversions, and a maximum of 65.98% with K<sub>1.5</sub>Mg/SiO<sub>2</sub> and TM<sub>0.3</sub> catalysts at a glucose conversion of 94.32% was achieved. This coincided with the trend that was for catalyst with relatively high base sites and Brønsted acid sites. Additionally, the high selectivity was attributed to the mesoporous structure of solid catalysts, which increased active sites of inner surface of catalysts. It was noted that lactic acid as a by-product was observed for all experiments due to the moderate base sites of K<sub>x</sub>Mg/SiO<sub>2</sub> catalyst.<sup>32,33</sup> The catalyst with K<sub>2</sub>MgSiO<sub>4</sub> component could have potential for the synthesis of lactic acid from glucose. From Table 1, it can be seen that glucose can be converted in the presence of the K<sub>1.5</sub>Mg/SiO<sub>2</sub> catalyst, and the selectivity of HMF was only 7% at 88% glucose conversion. In the absence of either the K<sub>1.5</sub>Mg/SiO<sub>2</sub> catalyst or TM<sub>0.3</sub> solid-acid, the yield of HMF was low (run 5 and 6). It could mean that the K<sub>1.5</sub>Mg/SiO<sub>2</sub> catalyst was in favor of the conversion of glucose, and TM<sub>0.3</sub> solid-acids with mesoporous structure helped improve the selectivity of HMF. The surface of TM<sub>0.3</sub> catalyst was in the presence of Lewis acid sites due to Ti<sup>4+</sup> and Si–O–Al bond of mordenite skeleton, and Brønsted acid sites were due to the sulphation process. The Lewis acid and Brønsted acid sites facilitated the dehydration reaction of fructose. The addition of K<sub>x</sub>Mg/SiO<sub>2</sub> catalysts improved significantly the conversion of glucose, as shown in runs 7–10, which led to an optimal HMF yield of 62.24% with a considerable reaction time. The

Table 1 Results of conversion of glucose and saccharides to HMF in a biphasic system

Run	Catalyst	Feedstock	Conversion of glucose (mole%)	Yield of HMF (mole%)	Selectivity of HMF (mole%)
1	K <sub>1.5</sub> Mg/SiO <sub>2</sub> + TM <sub>0.3</sub>	Enzymatic hydrolyzate	91.62	56.94	62.15
2	K <sub>1.7</sub> Mg/SiO <sub>2</sub> + TM <sub>0.3</sub>	Enzymatic hydrolyzate	81.45	47.59	58.43
3	K <sub>1.2</sub> Mg/SiO <sub>2</sub> + TM <sub>0.3</sub>	Enzymatic hydrolyzate	76.14	32.78	43.05
4	K <sub>1.0</sub> Mg/SiO <sub>2</sub> + TM <sub>0.3</sub>	Enzymatic hydrolyzate	52.78	33.36	63.2
5	K <sub>1.5</sub> Mg/SiO <sub>2</sub>	Glucose	88.17	7.58	8.6
6	TM <sub>0.3</sub>	Glucose	35.14	16.98	48.32
7	K <sub>1.5</sub> Mg/SiO <sub>2</sub> + TM <sub>0.3</sub>	Glucose	94.32	62.24	65.98
8	K <sub>1.7</sub> Mg/SiO <sub>2</sub> + TM <sub>0.3</sub>	Glucose	90.05	53	58.86
9	K <sub>1.2</sub> Mg/SiO <sub>2</sub> + TM <sub>0.3</sub>	Glucose	83.53	39.17	45.09
10	K <sub>1.0</sub> Mg/SiO <sub>2</sub> + TM <sub>0.3</sub>	Glucose	74.4	36.74	49.38
11	K <sub>1.5</sub> Mg/SiO <sub>2</sub> + TM <sub>0.3</sub> <sup>a</sup>	Glucose	70.3	34.6	49.22
12	K <sub>1.5</sub> Mg/SiO <sub>2</sub> + TM <sub>0.3</sub> <sup>b</sup>	Glucose	96.5	58.5	60.62

<sup>a</sup> Amount of K<sub>1.5</sub>Mg/SiO<sub>2</sub> catalyst was set to 0.3 g. <sup>b</sup> Amount of K<sub>1.5</sub>Mg/SiO<sub>2</sub> catalyst was set to 0.5 g.

Table 2 ICP-AES analysis of the fresh and used K<sub>1.5</sub>Mg/SiO<sub>2</sub> catalyst

	K (ppm)	Leaching ratio	Mg (ppm)	Leaching ratio
K <sub>1.5</sub> Mg/SiO <sub>2</sub> (fresh)	66.72 ± 0.5		13.36	
KMg-1	2.51 ± 0.5	3.76%	0.019	0.14%
KMg-2	1.79 ± 0.5	2.68%	0.016	0.12%
KMg-3	0.87 ± 0.5	1.3%	0.007	0.05%
KMg-4	0.38 ± 0.5	0.57%	0.007	0.05%
KMg-5	0.26 ± 0.5	0.39%	—	—
K <sub>1.5</sub> Mg/SiO <sub>2</sub> (used)	60.96 ± 0.5		13.25	

effectiveness of the K<sub>1.5</sub>Mg/SiO<sub>2</sub> catalyst for the conversion of glucose to fructose can be understood in terms of the intrinsic properties of base sites and dispersed rodlike microstructure. The product distribution was also influenced by the amount of the K<sub>1.5</sub>Mg/SiO<sub>2</sub> catalyst. Decreasing the amount of K<sub>1.5</sub>Mg/SiO<sub>2</sub> catalyst from 0.4 g to 0.3 g resulted in a declining yield of HMF (34%) with 49% selectivity, ascribed to a decrease in fructose formation by base-catalyzed isomerization (run 11). In contrast, increasing the amount of the K<sub>1.5</sub>Mg/SiO<sub>2</sub> catalyst to 0.5 g improved the HMF yield to 58% with 60% selectivity (run 12). It was very interesting to note that the moderate base sites and anisotropic structure would promote the aldose–ketose isomerization and the formation of lactic acid. Initially, the formation of D-fructose and D-mannose was observed. It was possible that the K<sub>1.5</sub>Mg/SiO<sub>2</sub> catalyst or Lewis acid sites promoted the isomerisation of D-glucose to the intermediate of D-mannose and D-fructose.<sup>34</sup> The formation of HMF could follow a mechanism, in which the open-chain form of fructose was dehydrated at the C-2 position using TM<sub>0.3</sub> solid acid, forming a carbocation which reacted with the hydroxyl group at C-5 position, forming furaldehyde intermediate followed by further dehydration to form HMF. Lactic acid, the main by-product, was likely formed from the hexoses *via* a complex reaction pathway without the formation of furaldehyde intermediate.<sup>32,35</sup> The first step was believed to consist of the formation of glyceraldehyde from the

saccharides through a retro-aldol condensation reaction. In a subsequent step glyceraldehyde was dehydrated to pyruvaldehyde, which subsequently rearranged to lactic acid.

### The stability of K<sub>1.5</sub>Mg/SiO<sub>2</sub> catalyst

The leaching test was designed to verify the stability of bonding potassium and magnesium of K<sub>1.5</sub>Mg/SiO<sub>2</sub> catalyst. In agreement with reaction conditions, 0.4 g catalyst was added into the water/butanol biphasic system and refluxed at 140 °C for 120 min. After reaction, water phase was separated from the reactor for a following analysis (mark as KMg-1). The solid catalyst was retained in the reactor for subsequent four leaching experiments according to the same procedure and the water phase samples of each step was marked as KMg-2, KMg-3, KMg-4 and KMg-5, respectively. Finally, the used catalyst was recovered for digestion and analysis. The amount of potassium and

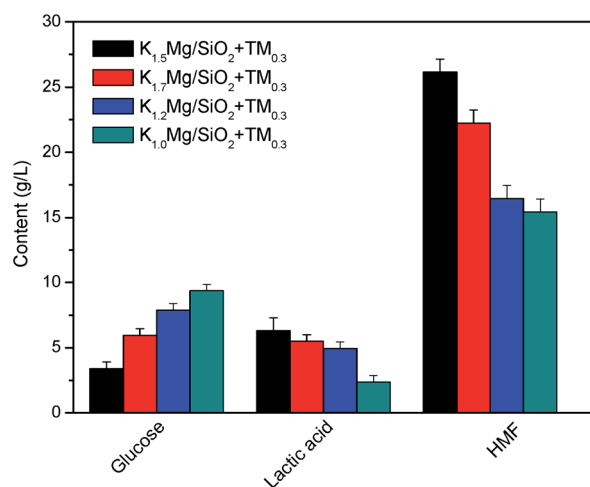


Fig. 5 Content of HMF and lactic acid resulted from the conversion of glucose by using different K<sub>x</sub>Mg/SiO<sub>2</sub> catalyst and TM<sub>0.3</sub> solid acids; reaction conditions: 6 wt% glucose aqueous solution at 140 °C for 180 min using 4 wt% K<sub>x</sub>Mg/SiO<sub>2</sub> catalyst and 6 wt% TM<sub>0.3</sub> catalysts, and organic to aqueous volume ratio of 3.

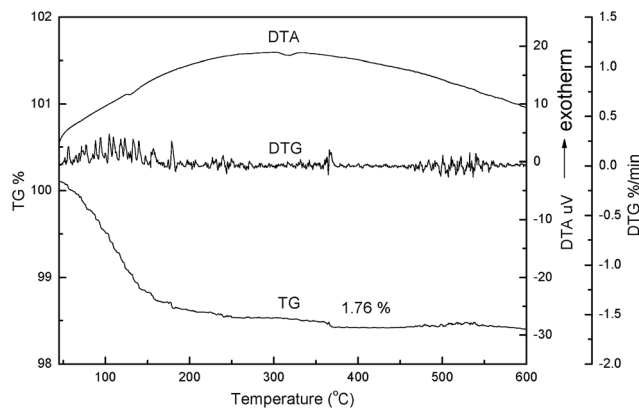


Fig. 6 TG-DTA curves of  $K_{1.5}Mg/SiO_2$  catalyst.

magnesium of prepared liquid samples were determined by ICP-AES. The analysis results (Table 2) showed that the content of K of the  $K_{1.5}Mg/SiO_2$  catalyst decreased slightly after each leaching test and the leaching ratio of potassium was less than 0.5% in the fifth cycle experiment. And the content of Mg maintained a constant after each leaching test, implying the stability of the  $K_{1.5}Mg/SiO_2$  catalyst. The low leaching ratio was correlated to the good reactivity of prepared catalyst corresponding to the high yield.

Further, the thermal behavior of the dried  $K_{1.5}Mg/SiO_2$  catalyst was shown in Fig. 6. Several ambiguous endothermic peaks were detected from on the DTA curve. The first endothermic peak is due to the release of adsorbed water of the catalyst sample around 150 °C resulting in 1.76% weight loss. The second peak at ca. 380 °C is attributed to the decomposition of the small amount of potassium nitrate. From TG plot, the weight remained almost unchanged above 600 °C, indicating the stability of the structure of solid catalyst.

Solid catalyst's stability played an important role in determining the economical application for large-scale production. The previous work<sup>36</sup> reflected massive potassium salt was soluble in the water of ethanol system and potassium leaching from the catalyst resulted in reducing the activity of catalyst. Here, using the silica gel as supporter is necessary to stabilize the active sites and to prevent the leaching procedure. The excellent catalytic properties confirmed that the components of the solid catalyst are synergetically assembled by the precipitation-gel-thermally activated process.

## Conclusions

Cost-effective conversion of saccharides from poplar sawdust to HMF was successfully conducted using a biphasic system in the presence of  $TM_{0.3}$  solid-acid and  $K_{1.5}Mg/SiO_2$  catalyst at a moderate reaction temperature. The integrating synthetic methodology offered the opportunity to utilize acid or base sites separately in a one-pot reaction system. The low leaching  $K_{1.5}Mg/SiO_2$  catalyst with moderate base sites could promote the aldose–ketose isomerization of glucose and has potential for the synthesis of lactic acid. The  $TM_{0.3}$  solid-acids with

mesoporous structure and strong Brønsted acid sites helped improve the selectivity of HMF. The one-pot catalysis of saccharides from enzymatic hydrolysate of poplar sawdust was in favor of low substrate concentration to avoid the competitive adsorption of oligosaccharides on solid catalysts. The optimal HMF yield of 56.9% at a glucose conversion of 91.6% was achieved for the complex saccharides system, which represented a considerable step toward the goal of developing a sustainable process for lignocelluloses conversion.

## Acknowledgements

This work is financially supported by the National Natural Science Foundation of China (40830748), the China Post-doctoral Science Foundation (201104497, 20090451092), the open foundation (CHCL10003) from MOE Key Laboratory of Catalysis and Materials Science of the State Ethnic Affairs Commission of Hubei in China and the Fundamental Research Funds for National University, China University of Geosciences (Wuhan) (Innovative Team, Grant CUG120115).

## Notes and references

- 1 M. FitzPatrick, P. Champagne, M. F. Cunningham and R. A. Whitney, *Bioresour. Technol.*, 2010, **101**, 8915–8922.
- 2 J. N. Chheda, G. W. Huber and J. A. Dumesic, *Angew. Chem., Int. Ed.*, 2007, **46**, 7164–7183.
- 3 G. Centi, P. Lanzafame and S. Perathoner, *Catal. Today*, 2011, **167**, 14–30.
- 4 R. S. Zalesny, R. B. Hall, J. A. Zalesny, B. G. McMahon, W. E. Berguson and G. R. Stanosz, *BioEnergy Res.*, 2009, **2**, 106–122.
- 5 Z. J. Wang, J. Y. Zhu, R. S. Zalesny and K. F. Chen, *Fuel*, 2012, **95**, 606–614.
- 6 M. Cantarella, L. Cantarella, A. Gallifuoco, A. Spera and F. Alfani, *Biotechnol. Prog.*, 2004, **20**, 200–206.
- 7 M. K. Bhat, *Biotechnol. Adv.*, 2000, **18**, 355–383.
- 8 P. Maki-Arvela, T. Salmi, B. Holmbom, S. Willfor and D. Y. Murzin, *Chem. Rev.*, 2011, **111**, 5638–5666.
- 9 P. L. Dhepe and R. Sahu, *Green Chem.*, 2010, **12**, 2153–2156.
- 10 Z. Fang, F. Zhang, H. Y. Zeng and F. Guo, *Bioresour. Technol.*, 2011, **102**, 8017–8021.
- 11 M. X. Cheng, T. Shi, H. Y. Guan, S. T. Wang, X. H. Wang and Z. J. Jiang, *Appl. Catal., B*, 2011, **107**, 104–109.
- 12 R. Kumar, G. Mago, V. Balan and C. E. Wyman, *Bioresour. Technol.*, 2009, **100**, 3948–3962.
- 13 Z. H. Zhang and Z. B. Zhao, *Bioresour. Technol.*, 2011, **102**, 3970–3972.
- 14 G. Gliozzi, A. Innorta, A. Mancini, R. Bortolo, C. Perego, M. Ricci and F. Cavani, *Appl. Catal., B*, 2014, **145**, 24–33.
- 15 S. De, S. Dutta, A. K. Parra, B. S. Rana, A. K. Sinha, B. Saha and A. Bhaumik, *Appl. Catal., A*, 2012, **435**, 197–203.
- 16 S. Zhao, M. X. Cheng, J. Z. Li, J. A. Tian and X. H. Wang, *Chem. Commun.*, 2011, **47**, 2176–2178.
- 17 H. F. Xiong, T. F. Wang, B. H. Shanks and A. K. Datye, *Catal. Lett.*, 2013, **143**, 509–516.

- 18 J. H. He, Y. T. Zhang and E. Y. X. Chen, *ChemSusChem*, 2013, **6**, 61–64.
- 19 Y. Roman-Leshkov, C. J. Barrett, Z. Y. Liu and J. A. Dumesic, *Nature*, 2007, **447**, 982–985.
- 20 J. P. Ma, Z. T. Du, J. Xu, Q. H. Chu and Y. Pang, *ChemSusChem*, 2011, **4**, 51–54.
- 21 J. M. R. Gallo, D. M. Alonso, M. A. Mellmer and J. A. Dumesic, *Green Chem.*, 2013, **15**, 85–90.
- 22 T. Buntara, S. Noel, P. H. Phua, I. Melian-Cabrera, J. G. de Vries and H. J. Heeres, *Angew. Chem., Int. Ed.*, 2011, **50**, 7083–7087.
- 23 Y. Yang, C. W. Hu and M. M. Abu-Omar, *Green Chem.*, 2012, **14**, 509–513.
- 24 Y. J. Pagan-Torres, T. F. Wang, J. M. R. Gallo, B. H. Shanks and J. A. Dumesic, *ACS Catal.*, 2012, **2**, 930–934.
- 25 Y. Roman-Leshkov, M. Moliner, J. A. Labinger and M. E. Davis, *Angew. Chem., Int. Ed.*, 2010, **49**, 8954–8957.
- 26 M. Moliner, Y. Roman-Leshkov and M. E. Davis, *Proc. Natl. Acad. Sci. U. S. A.*, 2010, **107**, 6164–6168.
- 27 E. Nikolla, Y. Roman-Leshkov, M. Moliner and M. E. Davis, *ACS Catal.*, 2011, **1**, 408–410.
- 28 X. Shen, Y. X. Wang, C. W. Hu, K. Qian, Z. Ji and M. Jin, *ChemCatChem*, 2012, **4**, 2013–2019.
- 29 M. S. Kotwal, P. S. Niphadkar, S. S. Deshpande, V. V. Bokade and P. N. Joshi, *Fuel*, 2009, **88**, 1773–1778.
- 30 D. Wang, X. Zhang, W. Wei and Y. Sun, *Catal. Commun.*, 2012, **28**, 159–162.
- 31 J. Di Cosimo, V. Díez, M. Xu, E. Iglesia and C. Apestegua, *J. Catal.*, 1998, **178**, 499–510.
- 32 X. Y. Yan, F. M. Jin, K. Tohji, T. Moriya and H. Enomoto, *J. Mater. Sci.*, 2007, **42**, 9995–9999.
- 33 A. Onda, T. Ochi, K. Kajiyoshi and K. Yanagisawa, *Catal. Commun.*, 2008, **9**, 1050–1053.
- 34 M. Watanabe, Y. Aizawa, T. Iida, R. Nishimura and H. Inomata, *Appl. Catal., A*, 2005, **295**, 150–156.
- 35 M. Bicker, S. Endres, L. Ott and H. Vogel, *J. Mol. Catal. A: Chem.*, 2005, **239**, 151–157.
- 36 G. Arzamendi, E. Arguiñarena, I. Campo, S. Zabala and L. M. Gandía, *Catal. Today*, 2008, **133–135**, 305–313.